



# OPEN Population-level shape variation and otolith asymmetry in *Diplodus annularis*

Spani Federica<sup>1,6</sup>, Kroha Silvio<sup>2,6</sup>, Scacco Umberto<sup>3,4</sup>, Di Giulio Andrea<sup>2,5</sup> & Scalici Massimiliano<sup>2,5</sup>

Sound detection in fishes relies on the inner ear and peripheral structures, such as calcareous otoliths, which play a crucial role in perceiving movement, orientation, and balance. Otoliths, in particular, respond to various environmental factors including temperature, salinity, and food availability, making them valuable indicators of ecological conditions. This study applies geometric morphometrics (GMM) to analyze the otolith shape of *Diplodus annularis* (Linnaeus, 1758) from two distinct populations located in the Gulf of Asinara (Porto Torres, Sardinia) and the northern Adriatic Sea (Le Tegnue). By using GMM techniques, precise and quantifiable differences in otolith morphology were revealed between the two populations, demonstrating significant shape variation. In addition, fluctuating asymmetry (FA), which serves as a marker for developmental stability and environmental stress, was assessed. The results show marked disparities in FA between the populations: samples from Porto Torres exhibited posterior asymmetry, while samples from Le Tegnue showed asymmetry in the anterior region of the otoliths. These findings underscore the sensitivity of GMM in detecting even subtle morphological differences, making it a powerful tool for studying environmental and genetic influences on marine species.

**Keywords** Mediterranean Sea, Sagittae, Geometric morphometrics, Intraspecific variation, Annular seabream.

Sound detection in fishes relies on the inner ear, and in certain species, additional peripheral structures that improve sound detection. The inner ear in fishes is similar to that of other vertebrates, containing three semicircular canals and three otolithic organs: the utricle, lagena, and saccule (see Fig. 1 in<sup>1,2</sup>). Otoliths are calcareous structures that move in response to gravitational forces or accelerations, stimulating the underlying hair cells and allowing the animal to perceive its position and movement. The otoliths of teleosts grow by the addition of concentric layers of calcareous crystals, the number of which can be used as an indication of the animal's age<sup>3</sup>. Moreover, otoliths exhibit characteristic shapes in different species and even among populations of the same species<sup>4,5</sup>. In fact, otoliths record information about the environmental context in which the fish lives, as their growth and composition can be influenced by various environmental factors such as water temperature, food availability, and the presence of pollutants<sup>6–16</sup>. Therefore, by studying the characteristics of otoliths, such as their shape and the composition of their layers, it is possible to obtain insights into environmental conditions and the variations that have occurred over time<sup>17–19</sup>.

Morphometry involves quantitatively describing, analyzing, and interpreting shape and its variations<sup>20</sup>, which has become a significant focus in biology. This has led to the development of various qualitative/quantitative and comparative analyses on anatomical structures, benefiting evolutionary biology and ecology studies<sup>21–24</sup>. Traditional morphometry, which considers aspects like lengths, widths, angles, and areas<sup>25</sup>, has limitations such as high autocorrelation of measurements and struggles in identifying causes for shape change<sup>26</sup>. This has spurred a revolution in morphometric investigation techniques since the early 1980s<sup>26,27</sup>. Strauss and Bookstein<sup>28</sup> highlighted the limitations of traditional approaches, emphasizing the importance of focusing on geometric relationships between variables based on ontogenetic models.

<sup>1</sup>Department of Science and Technology for Sustainable Development and One Health, Università Campus Bio-Medico di Roma, Via Alvaro del Portillo, Roma 21 - 00128, Italy. <sup>2</sup>Department of Sciences, University of Roma Tre, Viale Guglielmo Marconi, Roma 446 - 00146, Italy. <sup>3</sup>Istituto superiore per la Ricerca e Protezione Ambientale (ISPRA), National Center of Laboratories – Biology (CN-LAB-BIO), Via del Fosso Fiorano, Rome 64 - 00143, Italy.

<sup>4</sup>Department of Marine Biology and Ecology (DEBM), Università della Tuscia, Via S. Maria in Gradi, 4, Viterbo 01100, Italy. <sup>5</sup>National Biodiversity Future Center (NBFC), Università di Palermo, Piazza Marina, Palermo 61 – 90133, Italy.

<sup>6</sup>These authors contributed equally to this work. ✉email: f.spani@unicampus.it

### Von Bertalanffy Growth Model with 95% Confidence Interval – *D. annularis* Porto Torres

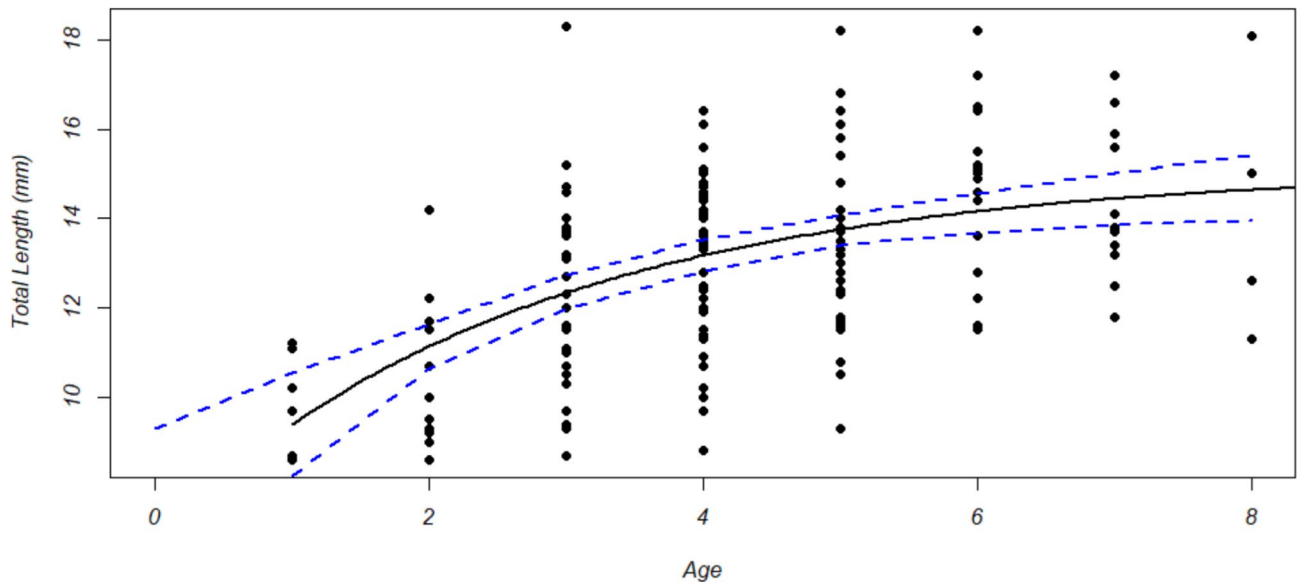


**Fig. 1.** Growth curve with 95% confidence interval for the *Diplodus annularis* population from Porto Torres. X-axis = age; Y-axis = total length.

#### Geometric morphometrics and otoliths

As the name suggests, geometric morphometrics (GMM) focuses on the geometric relationships of homologous points, known as landmarks, and has seen significant growth in usage in biological sciences, as evidenced by the increasing relevance of related keywords in scholarly searches. Its applications range from studying intraspecific and interspecific shape variability<sup>29,30</sup> to phylogeography<sup>31,32</sup> and surveys on biological structure asymmetry, which may indicate intrinsic or extrinsic perturbations in the ontogenetic process<sup>33</sup>. In this context, several authors have proposed fluctuating asymmetry as an indicator of either environmental or genetic stresses<sup>33,34</sup>. However, the presence of fluctuating asymmetry, at both the population and individual levels, does not necessarily imply an adaptive advantage. Conversely, other types of asymmetries, such as directional asymmetry and antisymmetry, are considered adaptive<sup>35</sup>. Geometric morphometrics has proven to be highly suitable for quantifying even minor variations and shape differences with greater accuracy when compared to traditional morphometric approaches<sup>36,37</sup>.

Various tools are available for analyzing geometric variables in two and three dimensions, using Cartesian coordinates of features like landmarks, curves, and outlines. These methods typically transform these features into shape coordinates, allowing for analysis using traditional statistical tools. Alternatively, some methods, such as Euclidean Distance Matrix Analysis (EDMA), transform data into a matrix of distances between variables. In geometric morphometrics landmarks are commonly used for shape analysis, employing Procrustes superimposition to standardize structures based on landmark positions, minimizing differences in orientation, position, and size for shape analysis<sup>38,39</sup>.

Different methods are used for analyzing curves and outlines. Semi-landmarks, positioned at intervals along curves between two landmarks<sup>40,41</sup>, are commonly employed for outline analysis, despite lacking biological meaning<sup>42</sup>. They are treated similarly to normal landmarks using Procrustes superimposition. Fourier analysis<sup>43</sup> describes outline coordinates using harmonic functions, while Eigenshape<sup>44–46</sup> converts coordinates into angle lists for analysis. However, outline/curve analysis is criticized for its lack of biological homology among single point coordinates<sup>47</sup>. On the other hand, using GMM with landmarks and semi-landmarks offers advantages over Fourier transformations in shape analysis<sup>36,37</sup>. GMM can detect even subtle shape variations<sup>36,37</sup> and is more intuitive for interpreting results. Unlike Fourier analysis, which distributes local shape information across multiple harmonic functions<sup>48</sup>, GMM enables decomposition into both global and local components of variation, facilitating graphical display and enhanced understanding of shape differences.

Traditional shape analyses of otoliths involve outline extraction techniques initially transformed into harmonic functions via Fourier transformation<sup>49–52</sup>. Over time, there's been a shift towards landmark-based analyses, refined with semi-landmarks for improved accuracy<sup>48,53–60</sup>. This transition has led to the adoption of GMM methods, emphasizing a reduced number of landmarks and semi-landmarks along otolith outlines. However, most GMM studies focus on shape discrimination rather than asymmetry. Palmer et al.<sup>61</sup> pioneered the use of GMM for studying otolith asymmetries, integrating landmarks ( $N=2$ ) and semi-landmarks ( $N=29$ ). Prior studies mainly relied on traditional morphometry<sup>62–65</sup> or outline transformation methods<sup>66–68</sup>.

### Von Bertalanffy Growth Model with 95% Confidence Interval – *D. annularis* Le Tegnue

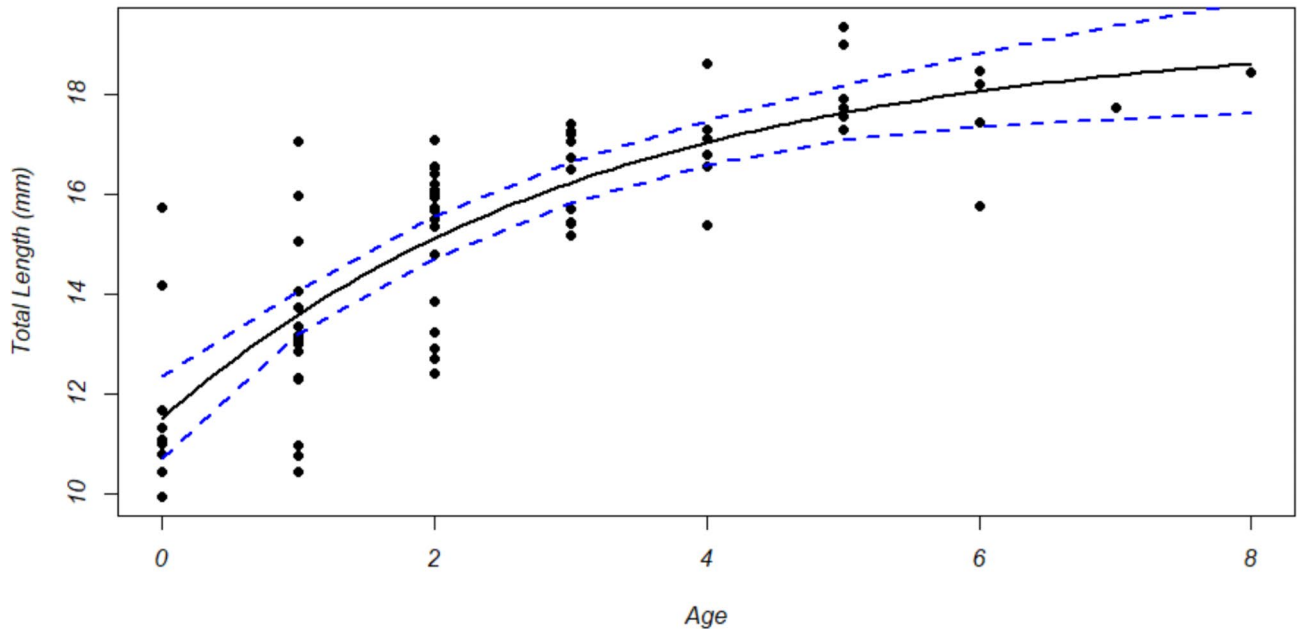


**Fig. 2.** Growth curve with 95% confidence interval for the *Diplodus annularis* population from Le Tegnue. X-axis = age; Y-axis = total length.

Growth Parameters for <i>D. annularis</i>						
Population	$L_{\infty}$	$p$ -value	K	$p$ -value	$t_0$	$p$ -value
Porto Torres	15.08	<2e-16	0.36	<b>0.0038</b>	-1.68	0.0735
Le Tegnue	19.21	<2e-16	0.32	<b>0.0010</b>	-2.89	<b>0.0001</b>

**Table 1.** Growth parameters of the Von Bertalanffy function for the two populations of *D. Annularis*.  $L_{\infty}$  = asymptotic length; K = growth coefficient;  $t_0$  = length at time 0.

### Background of the study and goals

This study is embedded within the broader framework of long-term marine monitoring initiatives led by ISPRA (Italian Institute for Environmental Protection and Research). ISPRA has been involved in various monitoring programs across the Mediterranean, aimed at assessing the status and trends of marine habitats and species. These programs have facilitated the collection of numerous *Diplodus annularis* (Linnaeus, 1758) specimens over time, providing a valuable resource for comparative morphological studies. The current study focuses on the detailed morphological analysis of otoliths in *D. annularis*, using geometric morphometrics (GMM) to assess shape variation and otolith fluctuating asymmetry (FA). Through a combination of landmark-based and outline analyses, this research aims to provide a comprehensive qualitative and quantitative framework for understanding otolith size, shape variation, and asymmetry in this species. Additionally, through the analysis of shape variation and otolith FA, two populations of *D. annularis* inhabiting two highly different environmental contexts will be compared. By leveraging advanced morphometric techniques, the study sets the groundwork for future shape-based comparisons and analyses of *D. annularis* populations.

### Results

#### Biological data: Von Bertalanffy growth curve

Differences in somatic growth between the two populations of *D. annularis* were analyzed using the Von Bertalanffy growth function and their associated parameters. Growth models were generated for the Porto Torres and Le Tegnue populations, with length plotted against age classes (Figs. 1 and 2). Resampling of the mean square errors was conducted to obtain frequency distributions of the growth parameters, which allowed for the calculation of confidence intervals.

In Table 1, the growth parameters of the Von Bertalanffy growth function for the two populations are presented, alongside their respective  $p$ -values. For the Porto Torres population, the asymptotic length ( $L_{\infty}$ , the theoretical maximum length an organism can reach) was 15.08 cm ( $p < 2e-16$ ), the growth coefficient (K, describing the rate at which the organism approaches its maximum length) was 0.36 ( $p = 0.0038$ ), and the theoretical age at which length is zero ( $t_0$ , the time offset to adjust the growth curve) was -1.68 ( $p = 0.0735$ ). For the Le Tegnue

population,  $L_{\infty}$  was 19.21 cm ( $p < 2e-16$ ),  $K$  was 0.32 ( $p = 0.0010$ ), and  $t_0$  was  $-2.89$  ( $p = 0.0001$ ). Assumptions of the growth model, including homoscedasticity, normal distribution of errors, model fit, and absence of significant outliers, were tested. Residual plots and histograms were used to evaluate these assumptions, with the results also presented in the supplementary materials.

### Geometric morphometrics: size analyses

In Fig. 3, the configurations of landmarks and semilandmarks relative to all samples belonging to the two studied populations are depicted (performed after the removal of identified outliers).

The size distribution of otoliths was analyzed through the creation of box plots (Supplementary Figures S1–S6) for the variables described in the subsection ‘Statistical analyses: morphometric data’ of Materials and Methods section. Regarding sex, analyses were only possible on a subsample of 46 individuals from Porto Torres, for whom sex was unambiguously determined. Out of 46 individuals, there were 15 females and 31 males. In the overall box plots generated on the dimensional data of otoliths, it is necessary to highlight (from a qualitative perspective) two different situations. The first is shown by comparing the distributions of otolith CSs between the two different populations (Porto Torres vs. Le Tegnue) where a difference was observed (Figure S4). The second is shown by the distribution of otolith CSs across different age classes, and within each class comparing right side with left side, which was performed for both Porto Torres (Figure S5) and Le Tegnue (Figure S6) populations. Both distributions clearly demonstrate dimensional growth along an age gradient, highlighting subtle but present differences between the left and right sides within the same age class.

In Table 2, the results of ANOVAs regarding CS of otoliths from the two populations are presented for the previously identified factors (significant differences are indicated in bold, setting  $p \leq 0.05$ ). A significant difference is observed in terms of age class for both populations ( $p < 0.02 * e^{-14}$ ), and between the two populations of *D. annularis* ( $p < 0.02 * e^{-14}$ ), and in terms of site for the combined sample of *D. annularis* ( $p < 0.02 * e^{-14}$ ). However, there is no significant difference regarding the sex factor, indicating the absence of dimensional sexual dimorphism.

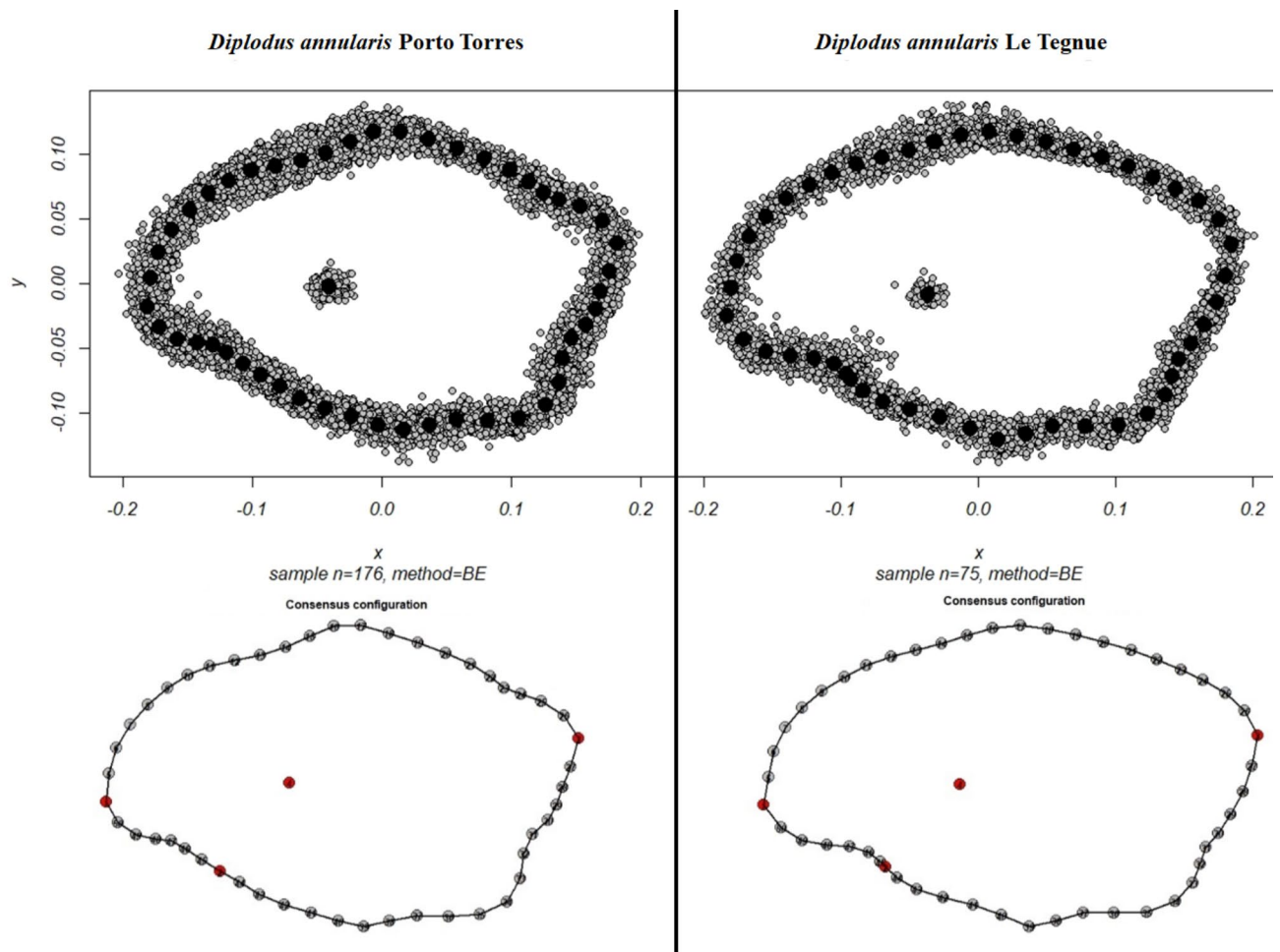


**Fig. 3.** Distribution of landmarks and semilandmarks (gray dots) fixed on all studied specimens (up) and their relative consensus configurations (black points, down) obtained for both populations of *Diplodus annularis* from Porto Torres (left) and Le Tegnue (right). BE = bending energy.

CS				
Species (site)	Age (yrs.)	Side	Sex	Site
<i>D. annularis</i> (PT)	<b>0.02*e<sup>-14</sup></b>	0.762	0.223	-
<i>D. annularis</i> (LT)	<b>0.02*e<sup>-14</sup></b>	0.432	na	-
<i>D. annularis</i> (PT + LT)	<b>0.02*e<sup>-14</sup></b>	0.873	na	<b>0.02*e<sup>-14</sup></b>

**Table 2.** *p*-values related to ANOVAs on the dimension data (CS = centroid size) of otoliths from the two populations of *Diplodus annularis*, with significant factors in bold, indicating a difference in size. Na = not available; LT = Le Tegnue; PT = Porto Torres.

Heterometry					
Species (site)	mCS	Age (yrs.)	Age classes	Sex	Site
<i>D. annularis</i> (PT)	0.39	0.143	<b>0.0299</b>	0.318	-
<i>D. annularis</i> (LT)	0.568	0.956	0.884	na	-
<i>D. annularis</i> (PT + LT)	0.305	0.888	0.357	na	0.77

**Table 3.** *p*-values related to ANOVAs on heterometry indices calculated individually for both populations of *Diplodus annularis*. Significant factors in bold. mCS = mean centroid size; na = not available; LT = Le Tegnue; PT = Porto Torres.

The figures from S7 to S12 depict the distribution of individual heterometry indices calculated in the studied populations in the form of box plots. Overall, deviations from the optimal condition were observed, with some cases of accentuated heterometry. When comparing populations (S7), subtle deviations from the optimal condition can be noted, with the presence of some outliers. Regarding sex differences (S8), females exhibit a wider distribution, indicating a higher degree of heterometry compared to males, who show a more concentrated distribution around the optimal condition. In analyzing the distribution by age class (S9 and S10), juvenile classes are more concentrated around the optimal condition compared to adult classes, which display greater variability and deviations from the optimal condition, especially in certain classes. For developmental stage (S11 and S12), juveniles exhibit a distribution more concentrated around the optimal condition, while adults have a greater number of outliers and substantial deviations from the optimal condition, although the difference between classes is not significantly appreciable. Following this (Table 3) are the results of the ANOVA pertaining to heterometry for the factors identified earlier (significant differences are indicated in bold, setting  $p \leq 0.05$ ). The only significant difference was observed for the age classes factor in the *D. annularis* population from Porto Torres ( $p = 0.0299$ ). There was no significant difference at the individual or site level, nor regarding otolith size or age class. Furthermore, regarding the sex factor (non-significant), the presence of heterometric sexual dimorphism can be excluded.

### Geometric morphometrics: shape analyses

Concerning the shape analysis, the result of principal component analysis for all samples is graphically represented in Fig. 4, with site used as the discriminating factor (Fig. 4-A). The goal was to identify clear groupings that reflect a sufficiently appreciable morphological distance between the two populations (PC1 = 23.4%; PC2 = 14.7%). In fact, two clusters were distinguished, corresponding to morphological diversity between the two populations of *D. annularis*. In terms of shape, individuals from Le Tegnue exhibit a less pronounced “bump” on the lower margin at the median position, and a longer rostrum, giving the sagittae a more streamlined shape. In the same figure (Fig. 4-B), the PCA regarding differences between sexes in the population from Porto Torres aiming to detect possible sexual dimorphism is presented (analysis performed on the subsample identified above). There is no clear spatial segregation between male and female individuals, suggesting an absence of sexual dimorphism even in terms of shape (PC1 = 27.8%; PC2 = 14.2%).

The abundance of age classes complicates the interpretation of the PCA plots obtained for the Porto Torres and Le Tegnue samples (Figures S13 and S14, respectively). However, regarding the Le Tegnue population, it is possible to observe that the younger classes are fairly clustered in the upper space of the Cartesian system, albeit displaying some degree of dispersion, while the older classes are particularly concentrated in the central/lower portion of the plot, showing a low degree of dispersion. The subsequent graphs, grouped by developmental stages, facilitate visual interpretation. In the Porto Torres population (Fig. 5-A), spatial segregation among the three classes was observed (PC1 = 25.3%; PC2 = 15.1%). Individuals not yet sexually mature primarily occupy the lower part of the Cartesian plane, while adults are found mainly in the upper part. Subadults show greater dispersion. The sagittae of young individuals are rounder with a convex lower margin and a short rostrum, whereas adults' sagittae have a concave lower margin and a more streamlined appearance. In the Le Tegnue population (Fig. 5-B), the graph grouped by developmental stages highlights the morphological proximity of adults and the dispersion of subadults (PC1 = 25.7%; PC2 = 16.9%). Again, spatial segregation among classes was observed, more pronounced for adults who are more closely clustered in the lower-left part of the Cartesian plane. Young individuals primarily occupy the upper-right part with less dispersion than adults do display. The

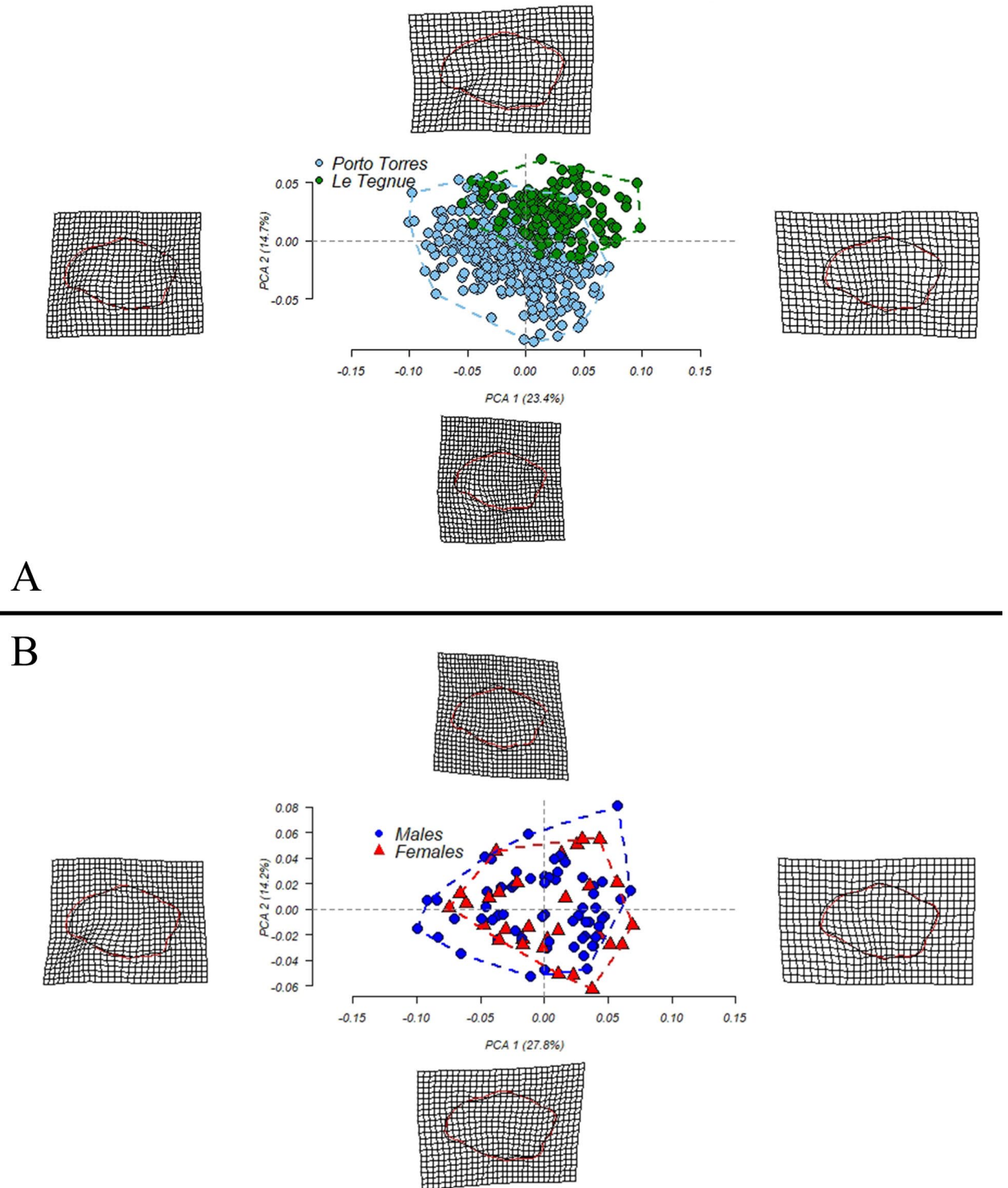


**Fig. 4.** A: Principal Component Analysis plot on the entire sample of *Diplodus annularis* using origin site as the discriminating factor, with associated deformation grids. B: Principal Component Analysis plot on the subsample of *Diplodus annularis* from Porto Torres using sex as the discriminating factor, with associated deformation grids.

sagittae of young individuals have a pronounced bump on the lower margin, while adults' sagittae have a flatter margin and a more streamlined appearance.

The ANOVAs conducted on the shape factors (Table 4) concerning the identified variables (see above) demonstrate an absence of sexual dimorphism in the shape of otoliths (Porto Torres population), consistent

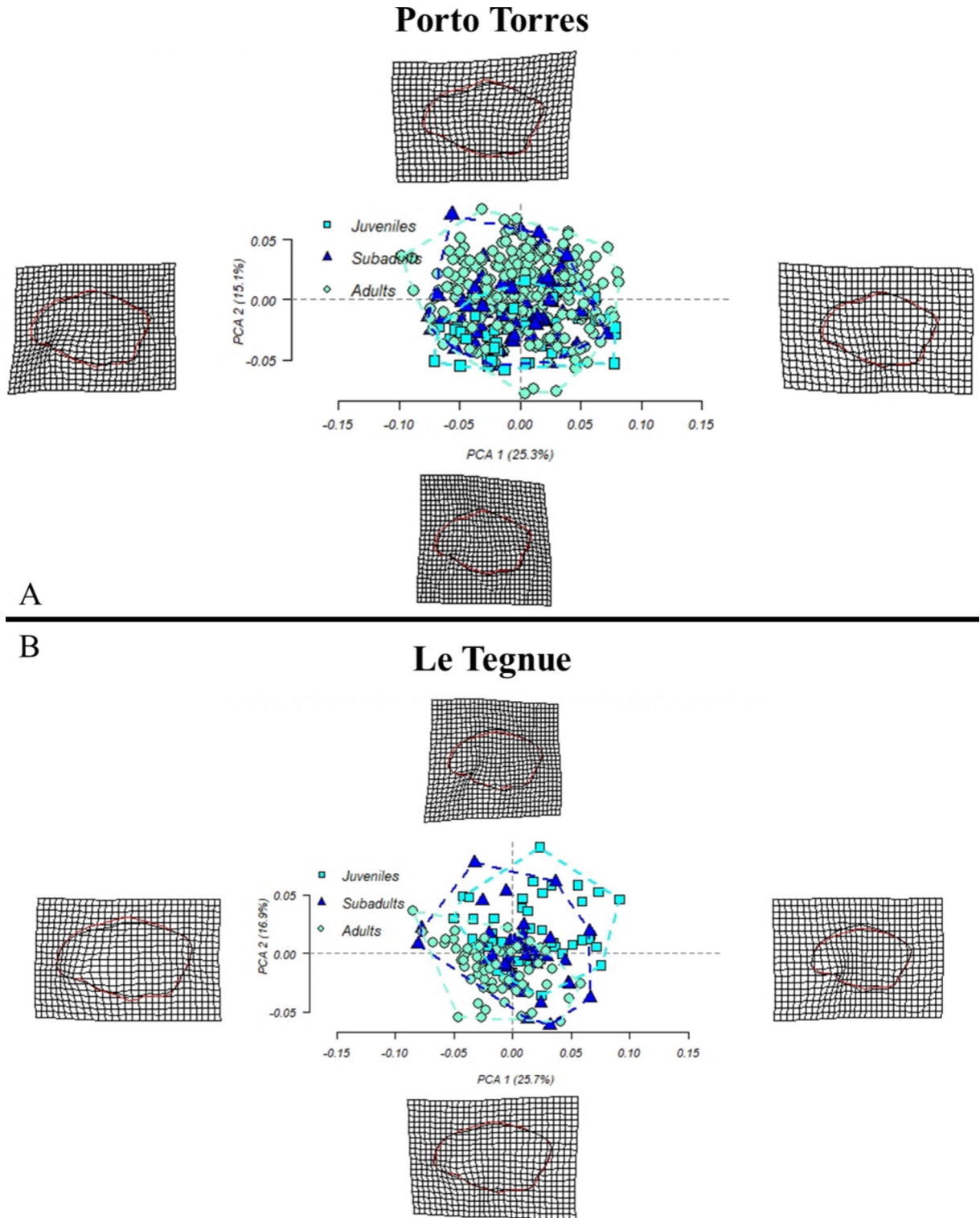


**Fig. 5.** Principal Component Analysis plots of the entire sample of *Diplodus annularis* from Porto Torres (A) and Le Tegnue (B) grouped by developmental stages with corresponding deformation grids.

with the previously observed lack of size dimorphism. However, significant shape differences were observed (in bold,  $p \leq 0.05$ ) when considering (1) age classes ( $p = 0.001$ ), (2) developmental stages ( $p = 0.001$ ), and (3) otolith size itself ( $p = 0.001$ ; although this variable is strongly autocorrelated with size), in both populations considered separately and together. Additionally, the shape difference between the two populations, considering the individuals' origin sites, was also found to be significant ( $p = 0.001$ ), as qualitatively highlighted earlier (see Fig. 4-A).

Species (site)	Shape				
	Age (yrs.)	Age classes	Sex	CS	Site
<i>D. annularis</i> (PT)	<b>0.001</b>	<b>0.001</b>	0.134	<b>0.001</b>	-
<i>D. annularis</i> (LT)	<b>0.001</b>	<b>0.001</b>	na	<b>0.001</b>	-
<i>D. annularis</i> (PT + LT)	<b>0.001</b>	<b>0.001</b>	na	<b>0.001</b>	<b>0.001</b>

**Table 4.** *p*-values related to ANOVAs conducted on shape factors. Significant factors are shown in bold. CS = centroid size; na = not available; LT = Le Tegnue; PT = Porto Torres.

Heteromorphy					
Species (site)	mCS	Age (yrs.)	Age classes	Sex	Site
<i>D. annularis</i> (PT)	0.503	0.809	0.629	0.601	-
<i>D. annularis</i> (LT)	0.323	0.0545	<b>0.0401</b>	na	-
<i>D. annularis</i> (PT + LT)	0.861	0.779	0.357	na	0.271

**Table 5.** *p*-values related to ANOVAs on heteromorphy indices calculated individually for both populations of *Diplodus annularis*. Significant factors in bold. mCS = mean centroid size; na = not available; LT = Le Tegnue; PT = Porto Torres.

The analysis of heteromorphy in the studied populations reveals that females (only for Porto Torres population) exhibit a more concentrated distribution and a slightly higher degree of heteromorphy when compared to males (S15). When examining the heteromorphy distribution by age classes and comparing the two populations (Porto Torres vs. Le Tegnue), a constant level of mean heteromorphy was observed in younger age classes, with an increase in adult stages and greater variability in both populations (Figs. S16, S18). Subsequently, heteromorphy decreases in older individuals, though this is evident only in the Porto Torres population (Figure S16) and not in Le Tegnue (Figure S18). Figures S17 and S19 depict heteromorphy levels grouped by developmental stage in both sites. In the Porto Torres population, a slight difference in mean heteromorphy levels was observed, with a trend towards increased variability in adult individuals (S17). Finally, in Figure S19, juvenile individuals exhibit the highest degree of variability, while subadults show the lowest variability and the lowest level of mean heteromorphy. Following, Table 5 presents the result of the ANOVAs regarding heteromorphy for the previously identified factors, with significant factors highlighted in bold. A significant difference was observed only for the developmental stage factor in the Le Tegnue population ( $p = 0.0401$ ). There was no significant difference at the individual or site level, nor regarding otolith size or age class. Furthermore, the sex factor was also not significant, thereby excluding the presence of heteromorphic sexual dimorphism.

The components of symmetric variation (i.e., directional asymmetry) and asymmetric variation (i.e., fluctuating asymmetry) of shape were used to disentangle and visualize the relative contribution of the two main types of asymmetry to the variation of shape itself. From the visual analysis of the deformation grids (Fig. 6), it is possible to infer a greater contribution of fluctuating asymmetry to the total component of asymmetric variation in both populations studied.

As a final analysis, an ANOVA was conducted on the spatial distribution of the FA component along the landmarks, considering the previously identified factors for both studied populations. Results are shown in Table 6. The only significant difference observed was between the *D. annularis* populations based on their site of origin (Porto Torres vs. Le Tegnue;  $p = 0.016$ ). This difference confirms what was already evident from the qualitative analysis of the previously examined deformation grids, but is now quantitatively confirmed by the performed ANOVA.

## Discussion

The study of otolith morphology has proven to be a powerful tool for understanding ecological and evolutionary patterns in fish species. Our results from the morphometric investigations are extremely interesting, demonstrating a significant and real difference in shape between the otoliths belonging to samples from Porto Torres and those from Le Tegnue. These differences manifest along two defined anatomical zones (see Fig. 7): one extending from the *ostium* (i.e., semilandmarks 45 to 50) of the *rostrum* (i.e., landmark 1), through the *collum* (the natural location of the auditory nerve involving the middle portion), directly adjacent to the *antirostrum* (i.e., landmark 2) on the dorsal margin. The other zone involves the area of the *postrostrum* (i.e., landmark 3) and the middle portion of the ventral margin. On average, samples from Le Tegnue have larger otoliths, a more concave channel (inflected *ostium*) and a wider *postrostrum* compared to samples from Porto Torres.

Differences between populations of the same species in different geographical areas are common among marine species<sup>69,70</sup>, particularly in osteichthyans<sup>71–76</sup>, including the species considered in this study, which belong to various areas of the Mediterranean<sup>77,78</sup>. For example, Bacha et al.<sup>79</sup> explored the relationships between age, growth, diet, and environmental parameters in *Engraulis encrasicolus* (Linnaeus, 1758) in the Mediterranean, revealing how these factors interact to shape the species' development. Similarly, Bose et al.<sup>80</sup> demonstrated congruent geographic variation in otolith shape across multiple African cichlid species, suggesting a strong link between environmental conditions and morphological variation.

Symmetric Shape component  
Directional asymmetry

Asymmetric Shape component  
Fluctuating asymmetry

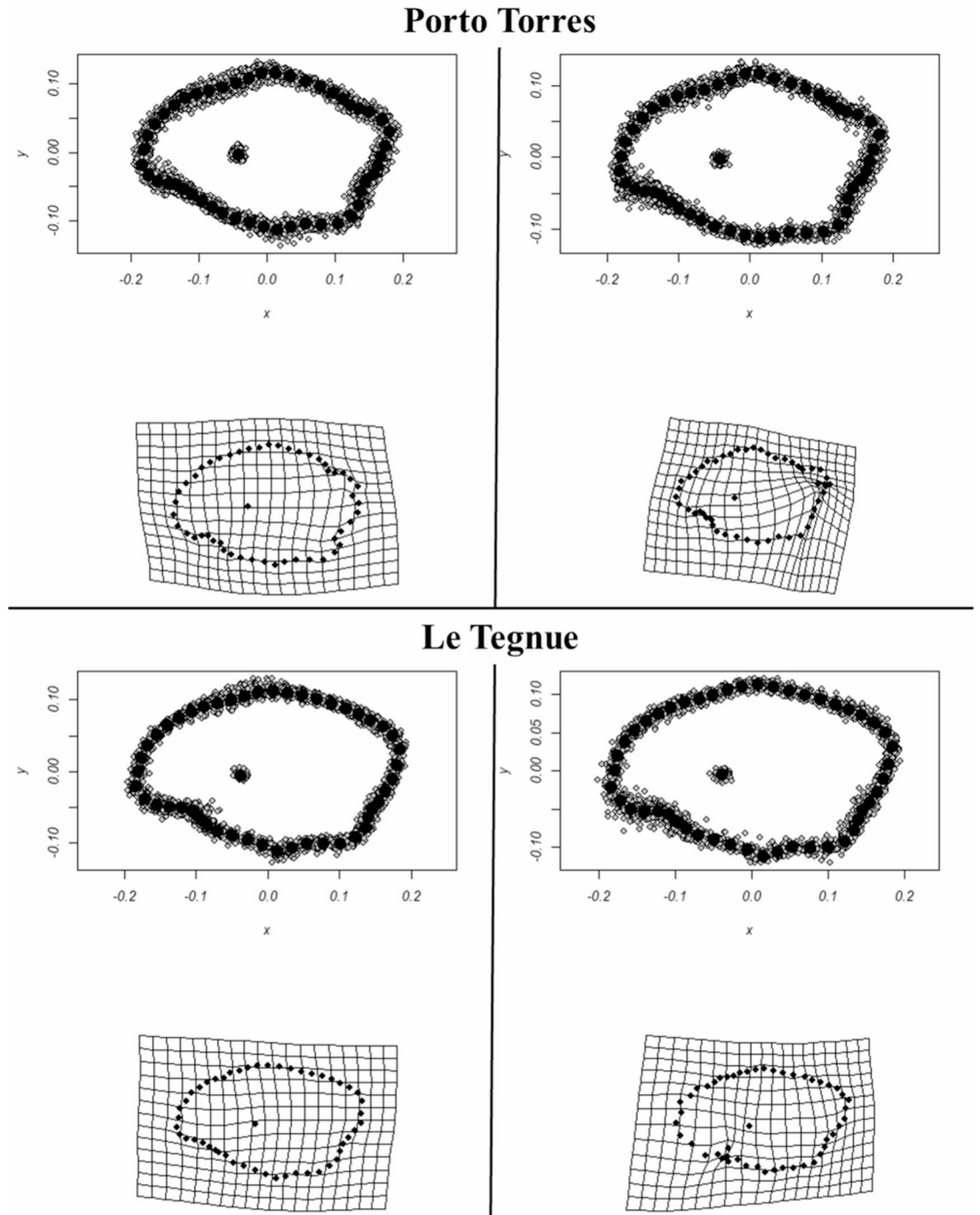


**Fig. 6.** Symmetric (left) and asymmetric (right) components of shape variation of otoliths at the individual level compared to consensus configurations (black dots), and relative deformation grids representing the contribution of directional and fluctuating asymmetry in the populations of *Diplodus annularis* from Porto Torres (above) and Le Tegnue (below).

Investigating the dimensional data of both right and left otoliths of each sample reveals no dimensional difference related to the side of the otolith or sex. Differences manifest concerning individual specimens and age and site groups. An expected result is related to growth: both otoliths significantly increase in size with age, especially in samples from Le Tegnue, which show larger otoliths than those belonging to samples from Porto

Fluctuating Asymmetry					
Species (site)	mCS	Age (yrs.)	Age classes	Sex	Site
<i>D. annularis</i> (PT)	0.41	0.557	0.792	0.306	-
<i>D. annularis</i> (LT)	0.991	0.148	0.986	na	-
<i>D. annularis</i> (PT + LT)	-	-	-	na	<b>0.016</b>

**Table 6.** ANOVA on the spatial distribution of the fluctuating asymmetry component calculated for both populations of *Diplodus annularis*. Significant factors are highlighted in bold. mCS = mean centroid size; na = not available; LT = Le Tegnue; PT = Porto Torres.

## Mean shape comparison *Diplodus annularis*

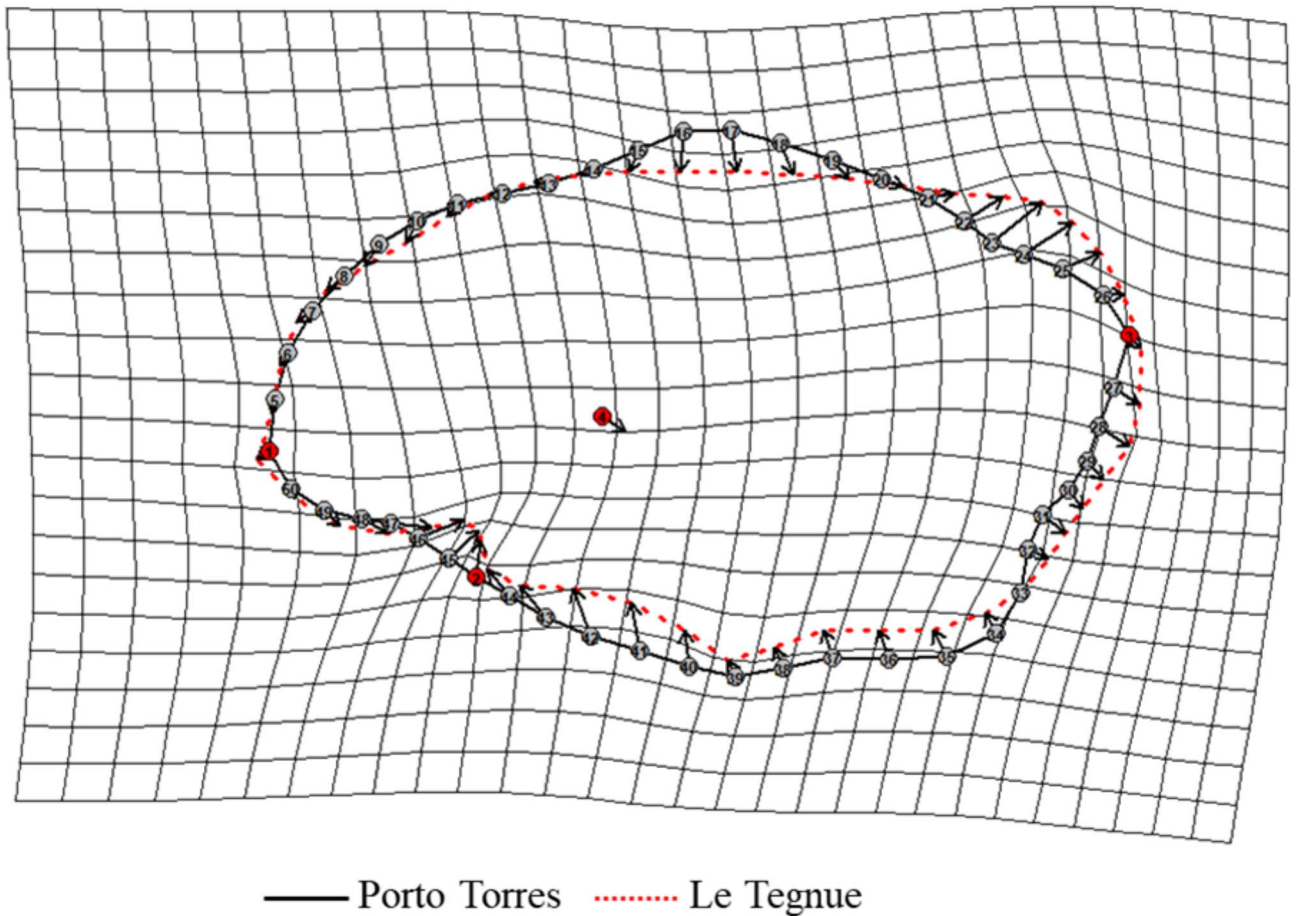


**Fig. 7.** Comparison between the mean shapes of *Diplodus annularis* otoliths from the two different sites with vectors indicating the direction of shape variation associated with each landmark (red) and semi-landmark (grey) pointing in the direction of shape variation.

Torres. However, concerning the heterometry index, it varies significantly only among growth groups in the sample from Porto Torres alone, with an increase in heterometry from young to adult individuals. Regarding the ontogenetic structure of shape differences in the two areas, interesting results also emerged concerning the distribution of data by sex, growth groups, and age. In this case, differences are structured according to a common shape gradient from juveniles to adults, with juveniles displaying differences attributable to the rostral zones compared to adults, where the areas of greater variability are found in the median portions of the upper and lower margins. The main difference between the two samples lies mainly in the orientation of the gradient, surprisingly opposite between Porto Torres and Le Tegnue samples. Considering the descriptive and quantitative results, the significance found for age, growth groups, otolith size, and site factors suggests a differing effect of

growth on otolith shape changes depending on the site. In fact, while in samples from Porto Torres, juveniles tend to have a more conservative shape compared to adults (with noticeable data dispersion), in samples from Le Tegnue the pattern is the opposite, where the only similarity is the considerable data dispersion observed for intermediate individuals, who exhibit a transitional shape between juveniles and adults. One possible explanation for these observations is the hypothesis that where trophic resources are a limiting factor (as in oligotrophic Sardinian waters), niche partitioning is stronger. Consequently, younger individuals, with a much narrower trophic spectrum than adults, become more competitive. Conversely, where trophic resources are never limiting (as in eutrophic Adriatic waters), niche partitioning could homogenize less competitive individuals (adults, with a much broader trophic spectrum than young ones) and offer more trophic “degrees of freedom” to juveniles, which would not undergo selection of a “mean” otolith shape. In fact, several studies support the notion that otolith shape can provide insights into species’ adaptation to different environments. For instance, D’Iglio et al.<sup>81</sup> investigated *Scorpaena porcus* Linnaeus, 1758, finding significant differences in otolith morphology and somatic growth rates between populations from different habitats, highlighting the role of ecological adaptation in shaping these traits. Cardinale et al.<sup>82</sup> further emphasized how factors such as sex, stock, and environment influence the otolith shape of Atlantic cod (*Gadus morhua* Linnaeus, 1758), providing a deeper understanding of population-specific traits. Mille et al.<sup>83</sup> also found that diet significantly influences otolith shape in marine fish, further supporting the idea that functional demands of feeding behavior are closely tied to morphological adaptations.

Regarding the heteromorphy index, it varies significantly only according to growth groups and only in the sample from Le Tegnue, with greater heteromorphy in adults and young individuals compared to the lower degree observed in subadults. In this case, the data does not seem to support what has already been discussed regarding shape variation patterns within the sample from Le Tegnue. In fact, if the eutrophy of the Adriatic site homogenizes the shape of adults more than it does for young individuals, the expected result for the right-left heteromorphy of adults should have shown the lowest value. Unfortunately, the lack of contrast in the comparison sample from Porto Torres does not allow us to fully support this hypothesis. Evidently, a trophic gradient, albeit pronounced, is reflected differently in heterometric and heteromorphic gradients. This observation is a reminder that size variations and shape variations are independent of each other, responding differently to internal and external organism conditions. Lombarte and Cruz<sup>84</sup> analyzed marine fish communities and observed that otolith size varied with depth (but see also<sup>16</sup>), indicating that environmental pressures such as temperature and depth play a significant role in shaping otolith morphology. In earlier work, Lombarte and Lleonart<sup>85</sup> had also established a link between otolith size and factors like body growth and habitat depth, reinforcing the importance of environmental factors in otolith development, confirmed later by Mejri et al.<sup>11</sup> and Deida et al.<sup>15</sup>. In our study, unfortunately, there was no access to the environmental data that have been used in similar studies. But for future studies, the inclusion of such data is desirable in order to carry out correlation analyses between the size and shape of otoliths, and different environmental parameters.

It is therefore important to always consider and analyze size and shape variables, independently, in morphometric studies, and synthetic indices such as heterometry and heteromorphy are a valid tool for identifying even general asymmetries.

The analysis of symmetric and asymmetric components of shape variation and individual levels of asymmetry has highlighted a prevalence of the fluctuating type over the directional type. In *D. annularis* from Porto Torres, the FA component concentrates in the posterior portion of the sagittae, around the postrostrum zone, while in the sagittae of samples from Le Tegnue, fluctuating asymmetry concentrates in the anterior regions and mainly involves the portion of the antirostrum. Therefore, as confirmed by quantitative tests, there is a difference between the two sampling sites regarding right-left heteromorphy, which topologically manifests in antipodal areas of the sagitta depending on the site but without showing differences in terms of magnitude. Furthermore, the results regarding the directionality of asymmetries are well explained in light of the ontogenetic results for shape variation. The samples seem to be pulled from opposite sides of the same morphological gradient (both in terms of heterometry and heteromorphy), one characterized by sagittal asymmetries concentrated anteriorly (a juvenile characteristic), the other with asymmetries concentrated more posteriorly (a characteristic of adults). This result tends to consolidate the idea that the right-left shape differences between the samples from the two sites are a stable and well-fixed characteristic in the populations from which the samples are drawn, probably due to prevalent ecological conditions of the sites of origin.

## Conclusions

In this study, we investigated the presence of asymmetries, with particular attention to fluctuating asymmetries, in a common marine fish species along the Mediterranean coasts. More generally, we described the shape variation associated with these structures during ontogeny and in relation to different ecological contexts, thus providing an initial understanding of population dynamics of *D. annularis* in the Gulf of Asinara area and the upper Adriatic Sea. Based on the results of qualitative and quantitative analyses, we can assert that bilaterally symmetric structures like otoliths well fit to geometric morphometric investigations, being able to identify even subtle asymmetries and provide an accurate description of shape variations in relation to observed variables (sampling site, species, sex, age).

The integration of studies on otolith shape analysis highlights that such methodologies are critical for stock discrimination. For instance, research on two insular populations of *D. annularis* from Tunisia demonstrated significant left-right asymmetries and sexual dimorphism in otolith morphology, supporting the hypothesis that otolith shape variations are influenced by both genetic and environmental factors<sup>86</sup>. Similarly, analysis of *D. vulgaris* otoliths from two Tunisian lagoons revealed marked fluctuating asymmetry, particularly in width and area parameters, reflecting environmental pressures such as salinity and temperature variations, as well as

anthropogenic impacts. These findings underline the role of fluctuating asymmetry as a potential indicator of developmental instability linked to habitat-specific stressors<sup>9</sup>.

This study confirmed the adequacy of the method for investigating morphological differences, especially regarding the ability to elucidate shape variations between two populations of the same species and within populations among biologically identified groups (sexes, developmental stages). The lack of direct measurements of stress indices, chemical and ecotoxicological analyses, in the two study areas, along with the absence of a significant difference in fluctuating asymmetry between the two studied populations, limits the formulation of cause-effect relationships between stress factors and levels of fluctuating asymmetry. This evidence does not allow us to assess the adequacy of otolith FA as an index of stress states and/or population success. In the specific case, however, we can conclude that fluctuating asymmetries are present and that the degree differs significantly between the two populations.

Furthermore, this study clearly highlights how shape is a conserved variable within individual stable evolutionary units such as populations and therefore attributable, in addition to genetics that determine its development and intrinsic variability, also to the ecological context from which individuals originate<sup>29</sup>. Consequently, shape also responds to factors that directly or indirectly contribute to its definition, such as anthropogenic pressures and stressors of various kinds<sup>69,70,87</sup>. The hypothesis regarding morphological variability suggests that environmental factors, such as water quality and nutrient levels, may influence the shape and structure of biological features, like otoliths or other morphological traits in marine species. The use of a trophic index, specifically the TRIX index<sup>88</sup>, could be highly beneficial in this context because it provides a quantitative measure of the trophic status of coastal marine waters. TRIX integrates four key parameters reflecting the nutrient levels, primary productivity, and potential for eutrophication in a given area. By applying the TRIX index to the study sites, researchers can more precisely characterize the environmental conditions under which the populations live. Incorporating TRIX data into the analysis of morphological variability could help determine whether differences in environmental quality, such as nutrient availability or productivity, are correlated with observed variations in morphological traits. This would provide a clearer understanding of how environmental factors influence the physical characteristics of marine organisms, making it easier to evaluate the hypothesis of morphology being shaped by environmental conditions. This study confirms the reliability of geometric morphometric methods in distinguishing morphological groups within a species. It suggests that these methods could be valuable for identifying fish stocks at the population or subpopulation level, particularly for migratory species or in areas where species have extensive distributions and there is high spatial overlap. Such information could aid in effective fisheries management strategies. It fits within a wide range of methodologies, often meticulous and susceptible to error introduction. Additionally, the ability to assess the presence of any directional asymmetries in otoliths is a necessary tool to avoid introducing bias in the process of discriminating fish stocks.

## Materials and methods

### Ethics declarations

The otoliths analyzed were extracted from fish that were already deceased; no fish were sacrificed for the purpose of this research. Additionally, the fish used in the study were not collected by us but were obtained from commercial fishing activities conducted by professional fishermen. All experimental protocols were approved by the Italian Institute for Environmental Protection and Research (ISPRA) as part of a monitoring plan associated with the installation of high-voltage submarine cables between Sardinia and mainland Italy, under the 'SAPEI' project (CIPE n. 144/2005, December 2). All methods were conducted in accordance with relevant guidelines and regulations and are reported in compliance with the ARRIVE guidelines.

### Study area

The primary study area for this research is the Gulf of Asinara, located in the municipality of Porto Torres, in northwestern Sardinia, Italy (40°51'47.66''N, 8°36'1.91''E; Fig. 8). The Gulf is part of a semi-enclosed basin influenced by Mediterranean currents and characterized by a mix of shallow coastal zones and deeper areas. The seafloor in the specific study area is dominated by degraded *Posidonia oceanica* meadows, composed primarily of dead rhizomes and detritus, resulting from both natural processes and anthropogenic impacts. These environmental conditions provide a unique habitat, which has undergone significant ecological changes, offering a valuable opportunity to investigate the morphological characteristics of otoliths in *D. annularis*. Long-term monitoring efforts by ISPRA (Italian Institute for Environmental Protection and Research), have further enriched the ecological understanding of this region.

A comparative study area in the northern Adriatic Sea, within the biological protected area of Le Tegnue, situated off the coast of Chioggia, near Venice, Italy (45°12'58.31''N, 12°33'24.57''E; Fig. 8). Le Tegnue is characterized by its complex benthic habitats, which include natural reefs and rocky substrates interspersed with sandy and muddy patches. These structures create a high level of habitat heterogeneity, supporting a rich diversity of marine life. The Adriatic Sea is a shallow basin with high nutrient input, influenced by freshwater inflows and strong hydrodynamic activity, which shape the local environmental conditions.

This dual focus on the Gulf of Asinara and Le Tegnue allows for a comparative analysis of otolith morphology in *D. annularis*, contributing to a broader understanding of how environmental variability influences shape variations in this species.

### Sampling

For both study areas, a fishery-independent sampling was conducted, meaning that researchers were present during sampling and controlled fishing operations. The otoliths analyzed were extracted from fish that were already deceased, and no fish were sacrificed by us for the purpose of this research. Furthermore, the fish

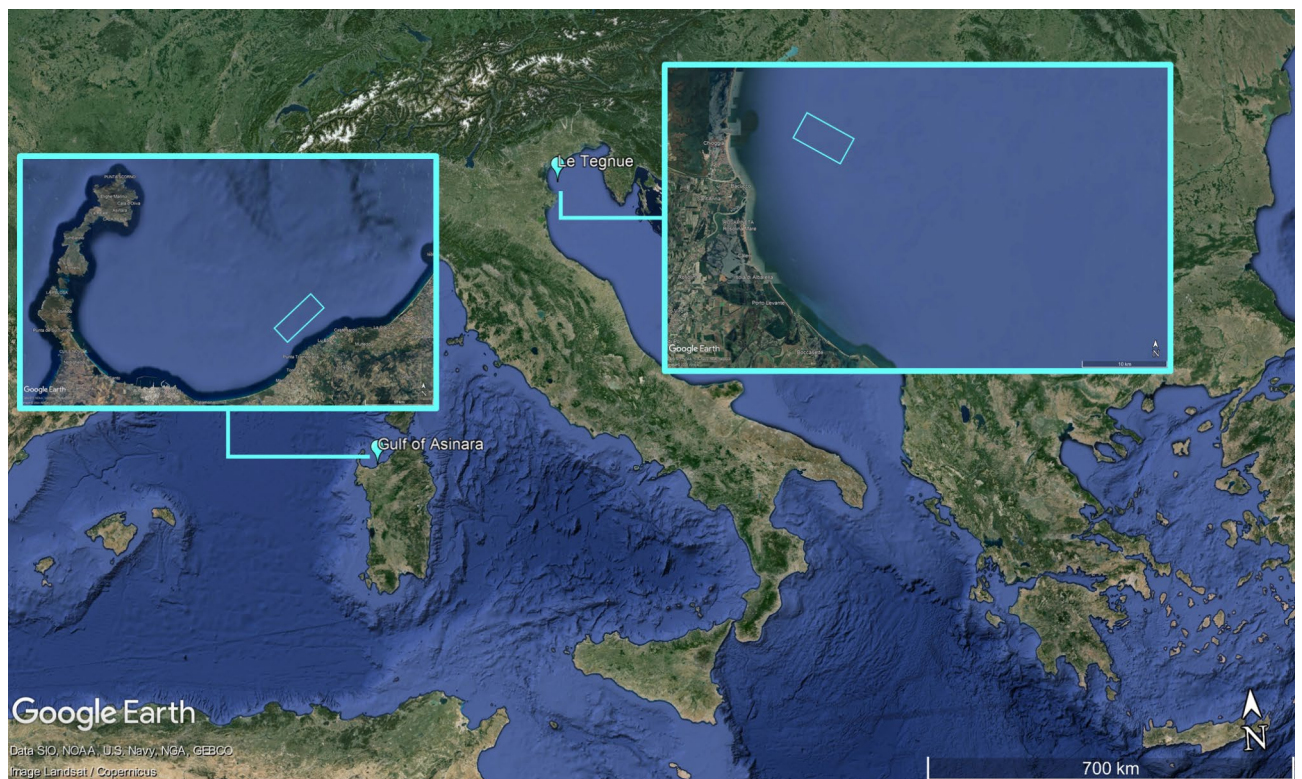


**Fig. 8.** Schematic representation of sampling areas (light blue squares) in the Gulf of Asinara (Porto Torres) and in the Adriatic Sea (Le Tegnue). Map created with Google Earth Pro (ver. 7.3, [https://www.google.co.uk/intl/en\\_uk/earth/](https://www.google.co.uk/intl/en_uk/earth/)) by FS.

used in the study were not collected by us but were obtained from commercial fishing activities carried out by professional fishermen. Concerning the primary study area of Porto Torres, sampling occurred seasonally from June 2017 to October 2018, and the choice of fishing gear (i.e., type and mesh size of the net) was made following a pre-survey conducted in the same area to measure capture effectiveness and selectivity. A “Barracuda” type gillnet made of three panels of different lengths, each with 2000 meshes: 50 m with 30 mm mesh, 30 m with 20 mm mesh, and 20 m with 15 mm mesh was chosen. Panels were deployed and repeated twice on the same frame for a total of 210 m including spacers of about 2 m between panels. Nets were deployed shortly before sunset and retrieved after a minimum of three hours. Fish were sorted onboard by mesh category, with basic biometric measurements taken (see below). Target species were stored in plastic bags with detailed information (i.e., study area, replicate, mesh, and individual progressive number) and frozen for transport to ISPRA laboratories. Sampling of *D. annularis* in the northern Adriatic Sea was conducted using methods comparable to those in Porto Torres, as both campaigns were part of ISPRA’s monitoring plans. However, it is important to clarify, for a better understanding of the subsequent analyses, that for the samples from the Porto Torres site, whole individuals were available, whereas for the samples from the Le Tegnue site, only extracted otoliths were available (as the sampling of individuals dates back to 2007). So, for the latter, the biological information on individual length was sourced from a historical and unpublished dataset (dated back to 2007). The combination of data collected during these two samplings allowed a robust morphological comparison of otoliths between *D. annularis* populations in the two study areas.

### Biological data collection

Specimens from Porto Torres were further processed by removing gonads, and sagittae (i.e., the large pair of otoliths) for subsequent analyses. Gonads were macroscopically classified by maturity stage and sex according to the guidelines of the Food and Agriculture Organization (FAO) for osteichthyans<sup>89</sup>, and the excised sagittae were rinsed in distilled water and stored dry until reading of growth rings. For age determination, sagittae (from both study areas) were placed on a microscope slide, immersed in glycerol, and growth patterns (annuli) were interpreted using a stereomicroscope based on available scientific literature<sup>90,91</sup>. Reading was preferably performed on the lateral surface (i.e., the opposite side of the mesial surface), starting from the *nucleus* towards the *rostrum* of the otolith, under white light as tangentially as possible to the curvature of the inner face of the otolith. If interpretation was ambiguous, the second otolith belonging to the same individual was also considered before reading from the mesial surface (see Fig. 9).

All otoliths were independently read by two expert researchers in the field (SK, US). Specimens were grouped by developmental stage following available literature on the sexual maturity degree of *D. annularis* belonging to those Mediterranean areas found to be as geographically and/or ecologically overlapping as possible with the

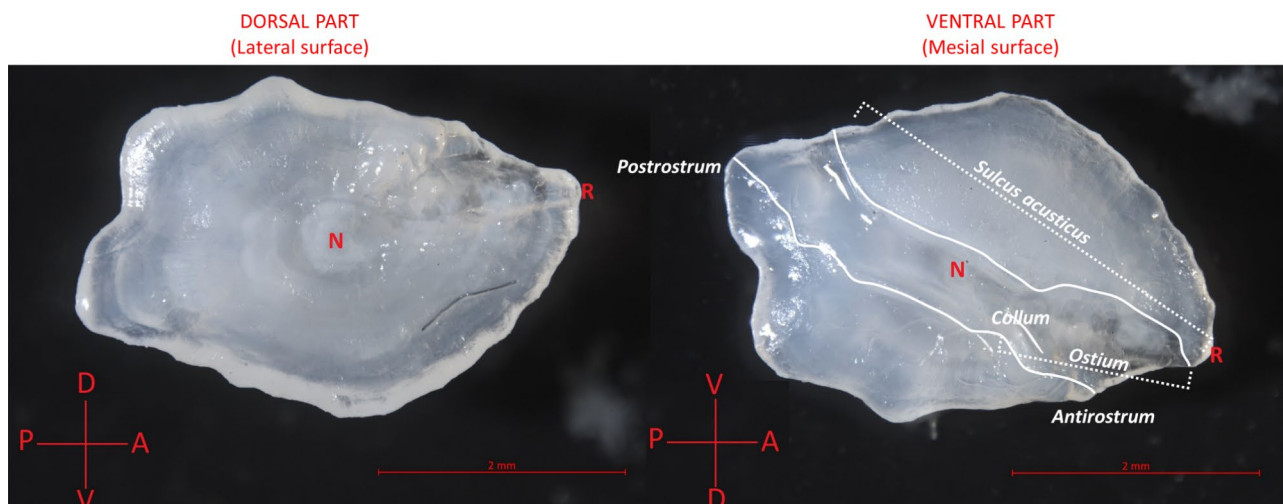


**Fig. 9.** Right otolith of *D. annularis*. On the left, lateral surface opposite to the sulcal side; on the right, mesial surface where the sulcal side is found. In white, main anatomical parts of otolith placed on the mesial surface. A = anterior; D = dorsal; N = nucleus; P = posterior; R = rostrum; V = ventral.

Porto Torres				Le Tegnue			
Age class	N	Development stage	N	Age class	N	Development stage	N
0+	0	Juvenile	21	0+	9	Juvenile	26
1	8			1	17		
2	13			2	19	Subadult	19
3	34	Subadult	34	3	11	Adult	30
4	46	Adult	121	4	6		
5	28			5	7		
6	24			6	4		
7	14			7	1		
8	5			8	1		
9	3			9	0		
10+	1			10+	0		
<b>Tot</b>	<b>176</b>		<b>176</b>		<b>75</b>		<b>75</b>

**Table 7.** Grouping by age classes and developmental stage of the *Diplodus annularis* sample from Porto Torres (left) and Le Tegnue (right).

two areas considered in this study<sup>78,92–94</sup>, as shown in Table 7 for specimens from Porto Torres and Le Tegnue, respectively. A total number of 176 individuals from Porto Torres and 75 from Le Tegnue were involved in the present study.

### Geometric morphometrics data collection

GMM data was collected only for individuals with intact sagittae (since they often proved difficult to extract due to their small size and fragility). Given the considerable thickness of the otoliths, in order to obtain suitable digital data in terms of sharpness and focus, the ZEISS Axio Zoom v16 multifocal microscope connected to a 3-megapixel AxioCam 503 microscope camera was used. A constant distance of 10  $\mu\text{m}$  between shots was maintained, resulting in a total of shots ranging from 50 to 150 for each otolith. Shots were subsequently overlapped applying the Extended Depth of Focus method, an image processing tool that aims at minimizing the distortion effect. Regarding the acquisition side, the mesial surface was chosen as the *sulcus acusticus* is useful for identifying homologous points where landmarks were positioned. For landmark positioning, the general approach of Palmer et al.<sup>61</sup> was followed, modified based on the most recent scientific literature. Using TPSdig2 (ver 2.32., <https://www.sbmorphometrics.org/index.html>), 4 true anatomical landmarks were manually positioned at clearly identifiable points on the otolith. In addition, 46 semi-landmarks were automatically generated along the otolith outline to capture its curvature. These semi-landmarks were distributed as follows: 8 equidistant points between landmarks 1 and 2, 18 between 2 and 3, 22 between 3 and 1. The software's automated function ensured consistent spacing and accurate representation of the otolith contour, reducing potential operator bias during semi-landmark placement. Figure 10 illustrates and describes the anatomical position of both landmarks and semi-landmarks on the acquired otoliths.

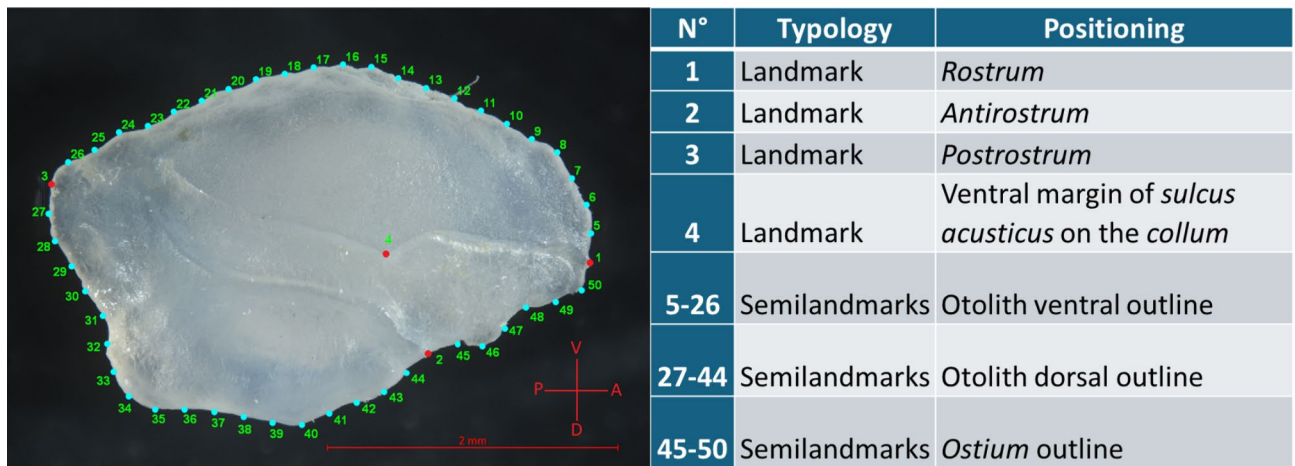


**Fig. 10.** Mesial surface of right otolith belonging to *Diploodus annularis* and landmarks/semilandmarks list, with their anatomical positions on the otolith. Red dots are landmarks; blue dots are semilandmarks. A = anterior; D = dorsal; P = posterior; V = ventral.

### Statistical analyses: biological data

Growth curves for *D. annularis* were constructed using the Von Bertalanffy growth equation, specifically following the Beverton-Holt parameterization:  $E[L|t] = L_{\infty} (1 - e^{-K(t-t_0)})$ . Initial estimates for  $L_{\infty}$  and  $K$  were obtained using the Ford-Walford graphical method based on mean age data. The initial value of  $t_0$  was estimated using a second-degree polynomial regression on mean length data for age classes<sup>95</sup>. Using these parameters, the Von Bertalanffy growth curve was fitted via nonlinear least squares minimization. The goodness of fit and confidence intervals for the estimated values were assessed through a bootstrap resampling process of the mean square errors. Additionally, frequency histograms of residuals were created, and actual model values were plotted against residuals to evaluate normality and homoscedasticity<sup>95</sup>.

For the *D. annularis* dataset from Le Tegnue, individual age readings, derived from growth rings, could not be directly linked to biometric data due to the absence of individual identification numbers at the time of database creation (i.e., it was impossible to link each individual to its biometric data). Assuming a linear correlation between otolith length and fish length<sup>96–99</sup>, a linear regression was performed on the mean otolith lengths of each pair against an equivalent number of randomly extracted total fish lengths from the original dataset, both ordered in ascending order. This analysis continued until the trend line in the “otolith length/total length” graph was significant for both the intercept and the slope, with an Akaike Information Criterion (AIC) not exceeding 35 (see supplementary figures S20–S24 for both graph and equation applied). The resulting equation was then used to calculate the expected lengths for each fish based on mean otolith length (which were subsequently used to construct the Von Bertalanffy growth curve, see above).

All ecological analyses were conducted using R, version 3.6.3 (R Core Team, 2013), with the assistance of the following packages: FSA<sup>100</sup>, dplyr<sup>101</sup>, nlstools<sup>102</sup>, AICcmoavg<sup>103</sup>, and basicTrendline<sup>104</sup>.

### Statistical analyses: geometric morphometrics data

Before conducting Procrustes superimposition<sup>27,105,106</sup>, adjustments were made to the images to ensure they were alignable. This involved mirroring half of the images (specifically, all right sides) by reversing the x-coordinate values of all landmarks. Following this, the images were scaled uniformly, centroids were aligned, and the images were rotated around the centroid to minimize distances between corresponding landmarks. Consequently, Procrustes shape variables were computed for each landmark and semilandmark, along with centroid size (CS), a dimensionless measure reflecting the otolith's size. To identify and remove outliers, Procrustes distances of each specimen were compared to the mean configuration of the entire sample, and consensus configurations were calculated, excluding outliers. Box plots were used to illustrate CS distribution across different variables: (1) side, (2) sex (only for *D. annularis* from Porto Torres), (3) site, and (4) age. Analysis of variance (ANOVA) was conducted to analyze dimensional data variability for these variables. Then, heterometry<sup>107</sup>, measuring the difference in size between bilateral structures, was calculated for each individual as the ratio between left and right CSs. As for CS, heterometry is a dimensionless measure as well. Box plots were generated to display the distribution of heterometry data across population, sex (only for *D. annularis* from Porto Torres), age, and developmental stage. ANOVA was performed considering these variables plus the mean CS ( $\frac{L_{otolith} + R_{otolith}}{2}$ ).

Shape variables obtained through Procrustes superimposition were employed for both qualitative and quantitative shape analyses. Principal component analysis (PCA) was used to discern any morphological affinity groups based on site, sex (specifically for *D. annularis* from Porto Torres), age, and developmental stage. Additionally, extremes of shape variation along principal axes were compared to a consensus configuration derived from all samples, aiding in visualizing shape differences. Hypothesis testing via ANOVA aimed to detect significant shape differences related to site, sex (only for *D. annularis* from Porto Torres), age, developmental stage, and CS. Heteromorphy<sup>107</sup>, an index reflecting shape diversity between bilateral structures, was calculated using

Procrustes distances between left and right sides of otolith, wherein a higher value of heteromorphy identifies a greater difference in form. Box plots were employed to visualize heteromorphy distribution by sex (only for *D. annularis* from Porto Torres), age (for both populations), and developmental stage (for both populations). As for CS and heterometry, heteromorphy is a dimensionless measure as well. Similar ANOVA analyses were conducted with CS as an additional variable. Directional asymmetry (DA) and fluctuating asymmetry (FA) components were calculated for the populations from both sites based on the symmetric and asymmetric components of shape variation around the mean. A mixed-model statistical framework was employed, including Procrustes ANOVA<sup>61</sup> for bilateral symmetries, and the multivariate extension of the univariate mixed model initially proposed by Leamy<sup>108</sup> and Palmer and Strobeck<sup>109</sup>. To visualize the symmetric and asymmetric shape variation components, a qualitative approach was used initially. Then, permutation-based variance tests were employed to identify differences in the spatial distribution of FA components across landmarks between populations. The tests considered additional variables such as site, age, developmental stage, sex (only for *D. annularis* from Porto Torres), and CS. All analyses were conducted in R (ver. 4.3.3) using packages including geomorph<sup>110,111</sup>, RRPP<sup>112</sup>, sp<sup>113</sup>, shapes<sup>114</sup>, and car<sup>115</sup>.

## Data availability

The raw data used in this study is available upon request to the corresponding author.

Received: 3 November 2024; Accepted: 16 January 2025

Published online: 20 January 2025

## References

- Popper, A. N. & Lu, Z. Structure–function relationships in fish otolith organs. *Fish. Res.* **46**, 15–25 (2000).
- Popper, A. N., Ramcharitar, J. & Campana, S. E. Why otoliths? Insights from inner ear physiology and fisheries biology. *Mar. Freshw. Res.* **56**, 497 (2005).
- Liem, K. F. *Functional Anatomy of the Vertebrates: An Evolutionary Perspective* (Harcourt College publ, 2001).
- Mille, T., Ernande, B., de Pontual, H., Villanueva, C. M. & Mahe, K. Sources of otolith morphology variation at the intra-population level: directional asymmetry and diet. (2016).
- D'Iglio, C. et al. Intra-population variability of the saccular, utricular and lagenar otoliths of the garfish *Belone belone* (Linnaeus, 1760) from South-Western Ionian Sea (Central Mediterranean Sea). *BMC Ecol. Evol.* **24**, 31 (2024).
- Schulz-Mirbach, T., Ladich, F., Plath, M. & Heß, M. Enigmatic ear stones: what we know about the functional role and evolution of fish otoliths. *Biol. Rev.* **94**, 457–482 (2019).
- Labidi, M. B. et al. Otolith fluctuating asymmetry in Boops boops (Actinopterygii, Sparidae) from two marine stations (Bizerte and Kelibia) in Tunisian waters. *J. Mar. Biol. Assoc. U.K.* **100**, 1135–1146 (2020).
- Labidi, M. B. et al. Stock discrimination of the bogue, Boops boops (Actinopterygii: Perciformes: Sparidae), from two Tunisian marine stations using the otolith shape. *Acta Ichthyol. Piscat.* **50**, 413–422 (2020).
- Khedher, M. et al. Discrimination of *Diplodus vulgaris* (Actinopterygii, Sparidae) stock from two Tunisian lagoons using otolith shape analysis. *J. Mar. Biol. Assoc. U.K.* **101**, 743–751 (2021).
- Mejri, M. et al. Interspecific and intersexual variability of the sagitta otolith shape between *Liza aurata* and *Chelon ramada* (Mugiliformes: Mugilidae) inhabiting the Boughrara lagoon, Tunisia. *Thalass Int. J. Mar. Sci.* **38**, 1357–1369 (2022).
- Mejri, M. et al. Discriminant Geographic Variation of Saccular Otolith Shape and size in the common Pandora, *Pagellus erythrinus* (Sparidae) across the Gulf of Gabes, Tunisia. *J. Ichthyol.* **62**, 1053–1066 (2022).
- Ben Mohamed, S. et al. Distinct inter and intrapopulation variation in the otolith shape and size of *Mullus barbatus* (Actinopterygii: Mullidae) from the Bizerte and Ghar El Melh lagoons in Tunisian waters. *Mar. Biol. Res.* **19**, 234–248 (2023).
- Houeto, M. F. A. et al. Discriminant inter and intrapopulation variation in sagittal otolith shape and morphometry in *Chelon ramada* (Actinopterygii, Mugilidae) from the Boughrara and El Bibane lagoons in Tunisian waters. *J. Mar. Biol. Assoc. U.K.* **104**, e13 (2024).
- Bakkari, W. et al. Distinctive morphological variation of saccular otoliths in relation to hermaphroditism type in *Sarpa salpa* and *Serranus scriba* (Teleostei: Perciformes) from the Mediterranean Sea in Bizerte, Tunisia. *Oceanol. Hydrobiol. Stud.* **53**, 261–276 (2024).
- Deida, T. et al. Do eco-geospatial differences induce otolith morphological variations? Assessment in *Chelon auratus* (Mugiliformes, Mugilidae) populations collected from Tunisian and Mauritanian waters. *J. Mar. Biol. Assoc. U.K.* **104**, e63 (2024).
- Mbadinga, K. C. M. et al. Intra and interspecies discrimination of three teleost species collected from the Komo Estuary in Gabon in relation to living depth levels using otolith shape analysis. *Mar. Biol. Res.* **20**, 288–303 (2024).
- Campana, S. E. Chemistry and composition of fish otoliths: pathways, mechanisms and applications. *Mar. Ecol. Prog. Ser.* **188**, 263–297 (1999).
- THORROLD, S. R., ZACHERL, D. C. & LEVIN, L. A. Population Connectivity and Larval Dispersal: using Geochemical signatures in calcified structures. *Oceanography* **20**, 80–89 (2007).
- Izzo, C., Reis-Santos, P. & Gillanders, B. M. Otolith chemistry does not just reflect environmental conditions: a meta-analytic evaluation. *Fish. Fish.* **19**, 441–454 (2018).
- Rohlf, F. J. & Morphometrics *Annu. Rev. Ecol. Syst.* **21**, 299–316 (1990).
- Gonzalez, P. N., Hallgrímsson, B. & Oyhenart, E. E. Developmental plasticity in covariance structure of the skull: effects of prenatal stress: developmental plasticity in covariance structure of the skull. *J. Anat.* **218**, 243–257 (2011).
- Soule, M. Phenetics of natural populations. II. Asymmetry and evolution in a Lizard. *Am. Nat.* **101**, 141–160 (1967).
- Møller, A. P. Developmental Stability and Fitness: a review. *Am. Nat.* **149**, 916–932 (1997).
- Frederich, B., Adriaens, D. & Vandewalle, P. Ontogenetic shape changes in Pomacentridae (Teleostei, Perciformes) and their relationships with feeding strategies: a geometric morphometric approach. *Biol. J. Linn. Soc.* **95**, 92–105 (2008).
- Proceedings of the Michigan Morphometrics Workshop*. University of Michigan Museum of Zoology, Ann Arbor, Mich, (1990).
- Parsons, K. J., Robinson, B. W. & Hrbek, T. Getting into shape: an empirical comparison of traditional truss-based morphometric methods with a newer geometric Method Applied to New World cichlids. *Environ. Biol. Fishes.* **67**, 417–431 (2003).
- James Rohlf, F. & Marcus, L. F. A revolution morphometrics. *Trends Ecol. Evol.* **8**, 129–132 (1993).
- Strauss, R. E. & Bookstein, F. L. The Truss: body form reconstructions in Morphometrics. *Syst. Biol.* **31**, 113–135 (1982).
- Scalici, M., Spani, F., Traversetti, L., Carpaneto, G. M. & Piras, P. Cranial shape parallelism in soft-furred sengis: moving on a geographic gradient. *J. Mammal.* <https://doi.org/10.1093/jmammal/gyy130> (2018).
- Spani, F., Morigi, M. P., Bettuzzi, M., Scalici, M. & Carosi, M. A 3D journey on virtual surfaces and inner structure of ossa genitalia in Primates by means of a non-invasive imaging tool. *PLOS ONE*. **15**, e0228131 (2020).

31. Gaubert, P., Taylor, P. J., Fernandes, C. A., Bruford, M. W. & Veron, G. Patterns of cryptic hybridization revealed using an integrative approach: a case study on genets (Carnivora, Viverridae, Genetta spp.) from the southern African subregion: CRYPTIC HYBRIDIZATION IN SOUTHERN AFRICAN GENETS. *Biol. J. Linn. Soc.* **86**, 11–33 (2005).
32. Cardini, A., Jansson, A. & Elton, S. A geometric morphometric approach to the study of ecogeographical and clinal variation in vervet monkeys. *J. Biogeogr.* **34**, 1663–1678 (2007).
33. Valen, L. V. A study of fluctuating asymmetry. *Evolution* **16**, 125–142 (1962).
34. Parsons, P. A. Fluctuating asymmetry: a biological monitor of environmental and genomic stress. *Heredity* **68**, 361–364 (1992).
35. Møller, A. P. & Swaddle, J. P. *Asymmetry, Developmental Stability and Evolution* (Oxford University Press, 1997).
36. Klingenberg, C. P., McIntyre, G. S. & GEOMETRIC MORPHOMETRICS OF DEVELOPMENTAL INSTABILITY: ANALYZING PATTERNS OF FLUCTUATING ASYMMETRY WITH PROCRUSTES METHODS. *Evolution* **52**, 1363–1375 (1998).
37. Zelditch, M. L., Wood, A. R. & Swiderski, D. L. Building Developmental Integration into Functional systems: function-Induced integration of mandibular shape. *Evol. Biol.* **36**, 71–87 (2009).
38. Rohlf, F. J. & Slice, D. Extensions of the Procrustes Method for the optimal superimposition of landmarks. *Syst. Zool.* **39**, 40 (1990).
39. Lawing, A. M. & Polly, P. D. Geometric morphometrics: recent applications to the study of evolution and development. *J. Zool.* **280**, 1–7 (2010).
40. Bookstein, F. L. Shape and the information in medical images: a decade of the morphometric synthesis. *Comput. Vis. Image Underst.* **66**, 97–118 (1997).
41. Bookstein, F. L. Landmark methods for forms without landmarks: morphometrics of group differences in outline shape. *Med. Image Anal.* **1**, 225–243 (1997).
42. Bookstein, F. L. *Morphometric Tools for Landmark Data.* (1997).
43. Younker, J. L. & Ehrlich, R. Fourier Biometrics: harmonic amplitudes as multivariate shape descriptors. *Syst. Biol.* **26**, 336–342 (1977).
44. Lohmann, G. P. Eigenshape analysis of microfossils: a general morphometric procedure for describing changes in shape. *J. Int. Assoc. Math. Geol.* **15**, 659–672 (1983).
45. MacLeod, N. & Rose, K. D. Inferring locomotor behavior in Paleogene mammals via eigenshape analysis. *Am. J. Sci.* **293**, 300–355 (1993).
46. MacLeod, N. Generalizing and extending the eigenshape method of shape space visualization and analysis. *Paleobiology* **25**, 107–138 (1999).
47. Zelditch, M. L., Fink, W. L. & Swiderski, D. L. Morphometrics, Homology, and Phylogenetics: quantified characters as synapomorphies. *Syst. Biol.* **44**, 179 (1995).
48. Vignon, M. & Morat, F. Environmental and genetic determinant of otolith shape revealed by a non-indigenous tropical fish. *Mar. Ecol. Prog Ser.* **411**, 231–241 (2010).
49. Bird, J. L., Eppler, D. T. & Checkley, D. M. Jr Comparisons of herring otoliths using Fourier series shape analysis. *Can. J. Fish. Aquat. Sci.* **43**, 1228–1234 (1986).
50. Castonguay, M., Simard, P. & Gagnon, P. Usefulness of Fourier analysis of otolith shape for Atlantic mackerel (*Scomber scombrus*) stock discrimination. *Can. J. Fish. Aquat. Sci.* **48**, 296–302 (1991).
51. Campana, S. E. & Casselman, J. M. Stock discrimination using otolith shape analysis. *Can. J. Fish. Aquat. Sci.* **50**, 1062–1083 (1993).
52. Begg, G. A. & Brown, R. W. Stock identification of haddock *Melanogrammus aeglefinus* on Georges Bank based on otolith shape analysis. *Trans. Am. Fish. Soc.* **129**, 935–945 (2000).
53. Monteiro, L. R., Benedetto, A. P. M. D., Guillermo, L. H. & Rivera, L. A. Allometric changes and shape differentiation of sagitta otoliths in sciaenid fishes. *Fish. Res.* **74**, 288–299 (2005).
54. Ponton, D. Is geometric morphometrics efficient for comparing otolith shape of different fish species? *J. Morphol.* **267**, 750–757 (2006).
55. Félix-Uraga, R. & Melo-Barrera, F. Using the shape of sagitta otoliths in the discrimination of phenotypic stocks in *Scomberomorus sierra* (Jordan and Starks, 1895). *J. Fish. Aquat. Sci.* **5**, 82–93 (2010).
56. Vignon, M. Ontogenetic trajectories of otolith shape during shift in habitat use: Interaction between otolith growth and environment. *J. Exp. Mar. Biol. Ecol.* **420–421**, 26–32 (2012).
57. de Carvalho, B. M., Vaz-dos-Santos, A. M., Spach, H. L. & Volpedo, A. V. Ontogenetic development of the sagittal otolith of the anchovy, *Anchoa tricolor*, in a subtropical estuary. *Sci. Mar.* **79**, 409–418 (2015).
58. Perez Quinonez, C., Quinonez Velazquez, C. & Garcia Rodriguez, F. Detecting *Opisthonema libertate* (Gunther, 1867) phenotypic stocks in northwestern coast of Mexico using geometric morphometrics based on body and otolith shape. *Lat Am. J. Aquat. Res.* **46**, 779–790 (2018).
59. Vignon, M. Short-term stress for long-lasting otolith morphology — brief embryological stress disturbance can reorient otolith ontogenetic trajectory. *Can. J. Fish. Aquat. Sci.* **75**, 1713–1722 (2018).
60. Salgado-Cruz, L., Quiñonez-Velázquez, C., García-Domínguez, F. A. & Pérez-Quinonez, C. I. Detecting *Mugil curema* (Perciformes: Mugilidae) phenotypic stocks in La Paz Bay, Baja California Sur, Mexico, using geometric morphometrics of otolith shape, growth, and reproductive parameters. *Rev. Mex. Biodivers.* **91**, 913273 (2020).
61. Palmer, M., Linde, M. & Morales-Nin, B. Disentangling fluctuating asymmetry from otolith shape. *Mar. Ecol. Prog Ser.* **399**, 261–272 (2010).
62. Somarakis, S., Kostikas, I., Peristeraki, N. & Tsimenides, N. Fluctuating asymmetry in the otoliths of larval anchovy *Engraulis encrasicolus* and the use of developmental instability as an indicator of condition in larval fish. *Mar. Ecol. Prog Ser.* **151**, 191–203 (1997).
63. Somarakis, S., Kostikas, I. & Tsimenides, N. Fluctuating asymmetry in the otoliths of larval fish as an indicator of condition: conceptual and methodological aspects. *J. Fish. Biol.* **51**, 30–38 (1997).
64. Fey, D. & Hare, J. Fluctuating asymmetry in the otoliths of larval Atlantic menhaden *Brevoortia tyrannus* (Latrobe)—a condition indicator? *J. Fish. Biol.* **72**, 121–130 (2008).
65. Kristoffersen, J. B. & Magoulas, A. Fluctuating asymmetry and fitness correlations in two *Engraulis encrasicolus* populations. *J. Fish. Biol.* **75**, 2723–2736 (2009).
66. Gagliano, M. & McCormick, M. Feeding history influences otolith shape in tropical fish. *Mar. Ecol. Prog Ser.* **278**, 291–296 (2004).
67. Mérigot, B., Letourneur, Y. & Lecomte-Finiger, R. Characterization of local populations of the common sole *Solea solea* (Pisces, Soleidae) in the NW Mediterranean through otolith morphometrics and shape analysis. *Mar. Biol.* **151**, 997–1008 (2007).
68. Lemberget, T. & McCormick, M. I. Replenishment success linked to fluctuating asymmetry in larval fish. *Oecologia* **159**, 83–93 (2009).
69. Scalici, M. et al. Using 3D virtual surfaces to investigate molluscan shell shape. *Aquat. Living Resour.* **29**, 207 (2016).
70. Scalici, M. et al. Integrated early warning systems in marine bivalves reveal detrimental alterations of coastal habitats. *Hydrobiologia* **847**, 2573–2585 (2020).
71. Jennings, S. & Beverton, R. Intraspecific variation in the life history tactics of Atlantic herring (*Clupea harengus* L.) stocks. *ICES J. Mar. Sci.* **48**, 117–125 (1991).
72. Present, T. M. C. & Conover, D. O. Physiological basis of Latitudinal Growth differences in *Menidia menidia*: variation in consumption or efficiency? *Funct. Ecol.* **6**, 23–31 (1992).

73. Shatunovskiy, M. I. & Ruban, G. I. Intraspecific variability of life strategies in boreal fishes inhabiting wide ranges. *Biol. Bull.* **37**, 413–422 (2010).
74. Caselle, J. E. et al. Geographic variation in density, demography, and life history traits of a harvested, sex-changing, temperate reef fish. *Can. J. Fish. Aquat. Sci.* **68**, 288–303 (2011).
75. Doubleday, Z. A. et al. Long-term patterns in estuarine fish growth across two climatically divergent regions. *Oecologia* **179**, 1079–1090 (2015).
76. Johnson, D. W., Stirling, B. S., Paz, J. & Satterfield, D. R. Geographic variation in demography of black perch (*Embiotoca jacksoni*): effects of density, food availability, predation, and fishing. *J. Exp. Mar. Biol. Ecol.* **516**, 16–24 (2019).
77. Gordoa, A. & Moli, B. Age and growth of the sparids *Diplodus vulgaris*, *D. sargus* and *D. annularis* in adult populations and the differences in their juvenile growth patterns in the north-western Mediterranean Sea. *Fish. Res.* **33**, 123–129 (1997).
78. Matic-Skoko, S., Kraljević, M., Dulčić, J. & Jardas, I. Age, growth, maturity, mortality, and yield-per-recruit for annular sea bream (*Diplodus annularis* L.) from the eastern middle Adriatic Sea. *J. Appl. Ichthyol.* **23**, 152–157 (2007).
79. Bacha, M. et al. Relationships between age, growth, diet and environmental parameters for anchovy (*Engraulis encrasicolus* L.) in the Bay of Bénisaf (SW Mediterranean, west Algerian coast). *Cybium* **34**, 47–57 (2010).
80. Bose, A. P. et al. Congruent geographic variation in saccular otolith shape across multiple species of African cichlids. *Sci. Rep.* **10**, 12820 (2020).
81. D'Iglio, C. et al. Ecomorphological adaptation of *Scorpaena porcus* (Linnaeus, 1758): evidence from two different environments revealed by sagittae features and somatic growth rates. *Front. Mar. Sci.* **11**, 1347897 (2024).
82. Cardinale, M., Doering-Arjes, P., Kastowsky, M. & Mosegaard, H. Effects of sex, stock, and environment on the shape of known-age Atlantic Cod (*Gadus morhua*) otoliths. *Can. J. Fish. Aquat. Sci.* **61**, 158–167 (2004).
83. Mille, T. et al. Diet is correlated with otolith shape in marine fish. *Mar. Ecol. Prog. Ser.* **555**, 167–184 (2016).
84. Lombarte, A. & Cruz, A. Otolith size trends in marine fish communities from different depth strata. *J. Fish. Biol.* **71**, 53–76 (2007).
85. Lombarte, A. & Lleonart, J. Otolith size changes related with body growth, habitat depth and temperature. *Environ. Biol. Fishes.* **37**, 297–306 (1993).
86. Trojette, M. Stock discrimination of two insular populations of *Diplodus annularis* (Actinopterygii: Perciformes: Sparidae) along the coast of Tunisia by analysis of otolith shape. *Acta Ichthyol. Piscat.* **45**, 363–372 (2015).
87. Cesarini, G. et al. Assessing teratogenic risks of gadolinium in freshwater environments: implications for environmental health. *Ecotoxicol. Environ. Saf.* **278**, 116442 (2024).
88. Vollenweider, R. A., Giovanardi, F., Montanari, G. & Rinaldi, A. Characterization of the trophic conditions of marine coastal waters with special reference to the NW Adriatic Sea: proposal for a trophic scale, turbidity and generalized water quality index. *Environmetrics* **9**, 329–357 (1998).
89. Bauchot, M. Poissons osseux. *Fiches FAO Identif. Pour Besoins Pêch. 1 Méditerranée. Mer Noire Zone Pêche.* **37**, 891–1421 (1987).
90. Abecasis, D. et al. Ageing seabreams: a comparative study between scales and otoliths. *Fish. Res.* **89**, 37–48 (2008).
91. Mouine, N., Ktari, M. H. & Chakroun-Marzouk, N. Age and growth of *Diplodus vulgaris* (Sparidae) in the Gulf of Tunis. *Cybium* **34**, 37–45 (2010).
92. Alós, J., Palmer, M., Alonso-Fernández, A. & Morales-Nin, B. Individual variability and sex-related differences in the growth of *Diplodus annularis* (Linnaeus, 1758). *Fish. Res.* **101**, 60–69 (2010).
93. Mouine, N., Francour, Ktari, M. H. & Chakroun-Marzouk, N. Reproductive biology of four *Diplodus* species *Diplodus vulgaris*, *D. annularis*, *D. sargus sargus* and *D. puntazzo* (Sparidae) in the Gulf of Tunis (central Mediterranean). *J. Mar. Biol. Assoc. U.K.* **92**, 623–631 (2012).
94. Ilkyazi, A. T., Metin, G., Soykan, O. & Kinacıgil, H. T. Spawning season, first maturity length and age of 21 fish species from the central Aegean Sea, Turkey. *Turk. J. Fish. Aquat. Sci.* **18**, 211–216 (2018).
95. Ogle, D. H. *fishR Vignette-Von Bertalanffy Growth Model-Extra*. In (Ashland (Northland College, 2013).
96. Harvey, J., Loughlin, T., Perez, M. & Oxman, D. Relationship between fish size and Otolith Length for 63 species of fishes from the Eastern North Pacific Ocean. *NOAA Tech. Rep. NMFS* **150**, 1–36 (2000).
97. Battaglia, P., Malara, D., Romeo, T. & Andaloro, F. Relationships between otolith size and fish size in some mesopelagic and bathypelagic species from the Mediterranean Sea (Strait of Messina, Italy). *Sci. Mar.* **74**, 605–612 (2010).
98. Jawad, L. A. et al. Rastrelliger kanagurta (CUVIER, 1817) COLLECTED FROM THE SEA OF OMAN. *Croat J. Fish. Ribar.* **69**, 51–61 (2011).
99. Khedher, M. & Fatnassi, M. Relationships between fish length otolith size of *Diplodus vulgaris* from Boughrara and El Bibane Lagoons (Southeastern Tunisia). *Res. Rev. J. Zool. Sci.* **6**, 43–50 (2018).
100. Ogle, D. H., Doll, J. C., Wheeler, A. P. & Dinno, A. *FSA: Simple Fisheries Stock Assessment Methods*. (2023).
101. Wickham, H., François, R., Henry, L., Müller, K. & Vaughan, D. *dplyr: A Grammar of Data Manipulation*. (2014). <https://doi.org/10.32614/CRAN.package.dplyr>
102. Baty, F. et al. A toolbox for nonlinear regression in R: the package nlstools. *J. Stat. Softw.* **66**, 1–21 (2015).
103. Mazerolle, M. J. *AICcmodavg: Model Selection and Multimodel Inference Based on (Q)AIC(c)*. (2023).
104. Mei, W. *basicTrendline: Add Trendline and Confidence Interval of Basic Regression Models to Plot. R Package Version 2.0.3*. (2018).
105. Adams, D. C., Rohlf, F. J. & Slice, D. E. Geometric morphometrics: ten years of progress following the 'revolution'. *Ital. J. Zool.* **71**, 5–16 (2004).
106. Slice, D. E. Geometric morphometrics. *Annu. Rev. Anthropol.* **36**, 261–281 (2007).
107. Spani, F., Scalici, M., Crandall, K. A. & Piras, P. Claw asymmetry in crabs: approaching an old issue from a new point of view. *Biol. J. Linn. Soc.* **blz159** <https://doi.org/10.1093/biolinnean/blz159> (2019).
108. Leamy, L. Morphometric studies in inbred and Hybrid House mice. V. Directional and fluctuating asymmetry. *Am. Nat.* **123**, 579–593 (1984).
109. Palmer, A. R. & Strobeck, C. Fluctuating asymmetry: measurement, analysis, patterns. *Annu. Rev. Ecol. Syst.* **17**, 391–421 (1986).
110. Adams, D. C., Collyer, M. L., Kaliontzopoulou, A. & Baken, E. K. Geomorph: Software for geometric morphometric analyses. R package version 4.0.9. (2024).
111. Baken, E. K., Collyer, M. L., Kaliontzopoulou, A. & Adams, D. C. Geomorph v4.0 and gmShiny: enhanced analytics and a new graphical interface for a comprehensive morphometric experience. *Methods Ecol. Evol.* **12**, 2355–2363 (2021).
112. Collyer, M. L. & Adams, D. C. RRPP: an r package for fitting linear models to high-dimensional data using residual randomization. *Methods Ecol. Evol.* **9**, 1772–1779 (2018).
113. Pebesma, E. J. & Bivand, R. Classes and methods for spatial data in R. *R News.* **5**, 9–13 (2005).
114. Dryden, I. L. *tt Shapes Package* (R Foundation for Statistical Computing, Vienna, 2021).
115. Fox, J. & Weisberg, S. *An R Companion to Applied Regression* (Sage, 2019).

## Acknowledgements

This research was supported by NBFC to the University of Roma Tre.

## Author contributions

E.S. and S.K. wrote the main manuscript text. U.S. and S.K. collected all samples. U.S. provided the unpublished

database. A.D.G. and S.K. acquired image data. S.K. performed all analyses. F.S. and M.S. supervised the project. All authors reviewed the manuscript.

## Declarations

### Competing interests

The authors declare no competing interests.

The authors declare that they have no known competing financial interests or personal relationships that could have appeared to influence the work reported in this paper.

**Tables.**

### Additional information

**Supplementary Information** The online version contains supplementary material available at <https://doi.org/10.1038/s41598-025-87096-3>.

**Correspondence** and requests for materials should be addressed to S.F.

**Reprints and permissions information** is available at [www.nature.com/reprints](http://www.nature.com/reprints).

**Publisher's note** Springer Nature remains neutral with regard to jurisdictional claims in published maps and institutional affiliations.

**Open Access** This article is licensed under a Creative Commons Attribution-NonCommercial-NoDerivatives 4.0 International License, which permits any non-commercial use, sharing, distribution and reproduction in any medium or format, as long as you give appropriate credit to the original author(s) and the source, provide a link to the Creative Commons licence, and indicate if you modified the licensed material. You do not have permission under this licence to share adapted material derived from this article or parts of it. The images or other third party material in this article are included in the article's Creative Commons licence, unless indicated otherwise in a credit line to the material. If material is not included in the article's Creative Commons licence and your intended use is not permitted by statutory regulation or exceeds the permitted use, you will need to obtain permission directly from the copyright holder. To view a copy of this licence, visit <http://creativecommons.org/licenses/by-nc-nd/4.0/>.

© The Author(s) 2025